Structural instabilities in $KTaO_3$ and $KNbO_3$ described by the nonlinear oxygen polarizability model

M. Sepliarsky, M. G. Stachiotti, and R. L. Migoni
Instituto de Física Rosario, Universidad Nacional de Rosario, 27 de Febrero 210 Bis, 2000 Rosario, Argentina
(Received 1 March 1995)

The validity of the nonlinear polarizability model to describe the different structural behavior as a function of temperature observed in $KTaO_3$ and $KNbO_3$ is analyzed. To this purpose, the total energy for different atomic distortions is evaluated and the results are compared with recent total-energy studies using *ab initio* methods. It is shown that the large O $2p$–Nb $4d$ hybridization observed in first-principles calculations and a model description through a nonlinear oxygen polarizability are actually not contradictory explanations for the origin of ferroelectricity in perovskites.

I. INTRODUCTION

The ABO_3 perovskites comprise one of the most important families of ferroelectric materials. Due to the simplicity of the structure and the wide variety of structural transitions that they display, they have attracted the interest of intense basic research over the past 50 years. These transitions are strongly dependent on the compound composition, i.e., the nature of the A and B ions in pure samples, as well as on the relative composition in mixed compounds. The different behavior of $KTaO_3$ and $KNbO_3$ can be taken as a very good example. While pure $KTaO_3$ is an incipient ferroelectric which does not undergo any phase transition, $KNbO_3$ undergoes a sequence of three phase transitions. With decreasing temperature it transforms from cubic paraelectric to tetragonal ferroelectric at 708 K, becomes orthorhombic at 498 K, and finally rhombohedral at 263 K.[1]

Numerous studies have been carried out in order to elucidate whether these transitions have a displacive or an order-disorder character. Initially, they were described in terms of a displacive model where a soft TO mode becomes unstable as the temperature is lowered, leading to displacements with the soft-mode eigenvector pattern.[2] This picture is supported by experiments showing softening phonon frequencies above the successive transitions.[3] However, many studies have presented results inconsistent with this soft-mode model and the eight-site model has been proposed.[3–8] According to this order-disorder model, the potential-energy surface has a maximum for the cubic perovskite structure and eight degenerate minima for the [111] displacements of the transition-metal ion that correspond to the low-temperature rhombohedral structure. In the cubic phase, the eight sites are occupied with equal probability, and this symmetry is broken as the temperature is lowered. Below 708 K, only four sites are occupied, which gives rise to a tetragonal symmetry; below 498 K, only two sites are occupied and the structure becomes orthorhombic and finally, below 263 K, only one site is occupied. The existence of such minima on the [111] directions has been confirmed by an extended x-ray-absorption fine structure (EXAFS) study,[9] model calculations,[10] and total-energy studies using the local density approximation.[11] On the other hand, the eight-site model cannot account for the observed phonon softening. While the pure soft-mode model and the eight-site model can be considered as limiting cases, most of the experimental data are consistent with a complicated combination of soft-mode and order-disorder behavior.

First-principles calculations have contributed greatly to understanding the origins of structural transitions in ferroelectric perovskites.[11–16] The results show that the hybridization between oxygen p and transition-metal d electrons is an important feature for driving the ferroelectric instability. On the other hand, phenomenological models—based on interatomic potentials—are also very useful to be used in simulation studies and they play an essential role in complementing a conceptual framework to a global understanding of ferroelectricity. The validity of any potential simulation study depends to a considerable extent on the quality of the pair potentials used, and there is an increasing interest in deriving pair potentials from *ab initio* calculations.

The lattice dynamics in the paraelectric phase of both $KTaO_3$ and $KNbO_3$, as well as the mixed compound $KNb_xTa_{1-x}O_3$, has been carried out in the framework of a nonlinear shell model. Indeed, as has been shown by Migoni *et al.*[17,18] on $KTaO_3$ and Kugel *et al.*[19,20] on the $KNb_xTa_{1-x}O_3$ system, the softening of the ferroelectric phonon mode is explained by a quartic and anisotropic core-shell coupling constant at the oxygen ion. The measured phonon-dispersion curves of $KTaO_3$, their temperature dependence, and the ones of $KNb_xTa_{1-x}O_3$ in the whole range of Nb concentrations have been well reproduced by only two concentration-dependent parameters which describe the linear and nonlinear oxygen polarizability. Then, as a main result, they have concluded that not only the temperature dependence of the soft mode but also its dependence on the Nb concentration is exclusively governed by the oxygen polarizability. However, for the calculation of these temperature-dependent properties, they made use of the self-consistent phonon approximation. This corresponds to a temperature-dependent linearization of the nonlinear potential: the

0163-1829/95/52(6)/4044(6)/$06.00

fourth-order term is replaced by an effective harmonic one, to be determined self-consistently. For this reason, the nonlinear polarizability model has wrongly been considered as a pure soft-mode model. A recent molecular dynamics simulation—using a two-dimensional version of the nonlinear polarizability model—allows us to account for the experimentally observed crossover from the displacive soft-mode picture to order-disorder dynamics near the transition.[21]

The aim of the present work is to clarify the validity of the nonlinear polarizability model to describe the different behavior observed in $KTaO_3$ and $KNbO_3$. It is not obvious at all that the proposed model, which has been determined to explain the lattice dynamics in the cubic phase, describes the peculiar displacement pattern dependence of the total energy which leads to the three successive phase transitions experimentally observed in $KNbO_3$. To this purpose, the underlying static potential for different atomic distortions is evaluated without linearization schemes, such as the self-consistent phonon approximation. The results are tested by comparing with recent model calculations[10] and total-energy studies using the local density approximation.[11] Finally, the relationship between the anomalous oxygen polarizability and the transition-metal–oxygen *d-p* hybridization is discussed.

II. MODEL AND COMPUTATIONAL DETAILS

In our calculations we have used the three-dimensional nonlinear polarizability model originally proposed to explain the ferroelectric behavior in oxide perovskites.[17] The K^+ ion and the Ta^{+5} or Nb^{+5} ions are considered isotropically polarizable. However, an anisotropic core-shell interaction is considered for the O^{-2} ion, since the oxygen polarizability depends strongly on the crystal environment. This anisotropy is described by two different linear coupling constants k_{OA} (in the direction of the K^+) and k_{OB} (in the direction of the Ta^{+5} or Nb^{+5} ions). The nonlinear fourth-order contribution is taken into account by a coupling constant $K_{OB,B}$ which acts only in the direction of the B ion.

All interionic interactions are taken of the long-range Coulomb type, except for the short-range forces that couple the oxygen shells to the ones of the nearest A^+, B^{+5}, and O^{-2} ions. These interactions are treated in the harmonic approximation, with the additional fourth-order term $k_{OB,B}$ in the core-shell coupling for the oxygen ion. Then, the model potential energy can be written as

$$V(\mathbf{u},\mathbf{v})=\frac{1}{2}\mathbf{u}^{\dagger}(\mathcal{S}+\mathcal{C}^{ZZ})\mathbf{u}+\frac{1}{2}(\mathbf{v}-\mathbf{u})^{\dagger}(\mathcal{S}+\mathcal{K}_2+\mathcal{C}^{YY})(\mathbf{v}-\mathbf{u}) +\mathbf{u}^{\dagger}(\mathcal{S}+\mathcal{C}^{ZY})(\mathbf{v}-\mathbf{u})+\frac{1}{4!}k_{OB,B}\mathcal{L}(\mathbf{v}-\mathbf{u})^4 , \quad (1)$$

where $\mathbf{u}$ and $\mathbf{v}$ denote core and shell displacements, respectively. $\mathcal{S}$ is the short-range force-constant matrix and $\mathcal{C}^{ij}$ represent the Coulomb matrices for interactions between ions ($\mathcal{C}^{ZZ}$), between shells ($\mathcal{C}^{YY}$), and between ions and shells ($\mathcal{C}^{ZY}$), Z denoting ionic charge and Y shell charge. $\mathcal{K}_2$ is a diagonal matrix which contains the linear core-shell coupling constants and the matrix $\mathcal{L}$ selects the appropriate components for the nonlinear interaction at the O^{-2} ions.

The values of the model parameters for $KTaO_3$ were obtained in Ref. 18 by a fit to experimental dispersion curves. Shell-model calculations with these parameters reproduce the measured phonon-dispersion curves and Raman spectra of $KTaO_3$ at room temperature and also the most significant temperature dependences of phonon frequencies from 0 to 1200 K, including that of the ferroelectric soft mode, within the self-consistent phonon approximation. As only little variation in phonon frequencies is observed when Nb is introduced in $KTaO_3$, except for the soft mode, Kugel *et al.*[19] have described the phonon-dispersion curves in the whole range of Nb concentration between 0% and 100% with only two concentration-dependent parameters: k_{OB} and $k_{OB,B}$. They found that while the linear constant k_{OB} decreases slightly from $340(e^2/v)$ (pure $KTaO_3$) to $270(e^2/v)$ (pure $KNbO_3$), the nonlinear parameter $k_{OB,B}$ increases drastically from about $2.4\times10^4(e^2/v\text{Å}^2)$ to $5.6\times10^4(e^2/v\text{Å}^2)$. This reflects the fact that the variation of the Nb-O distance produces a stronger variation of the oxygen polarizability than that of the Ta-O distance.

To evaluate the underlying static potential for the ferroelectric distortions, we have calculated the potential energy of the model for several atomic displacements. For a given set of homogeneous core displacements $\mathbf{u}$, we have evaluated the corresponding shell displacements (which represent the electronic degrees of freedom) by solving the adiabatic condition:

$$(\mathcal{S}+\mathcal{C}^{yz})\mathbf{u}+(\mathcal{S}+\mathcal{K}_2+\mathcal{C}^{yy})\mathbf{w}+\frac{1}{3!}k_{OB,B}\mathcal{L}(\mathbf{w})^3=0 , \quad (2)$$

where $\mathbf{w}=\mathbf{v}-\mathbf{u}$ are the relative shell-core displacements. Once the equilibrium solution for $\mathbf{w}$ is obtained iteratively from Eq. (2) by a steepest-descent procedure, the potential energy of the model is computed according to Eq. (1).

Since the previous works[17–20] specify only the harmonic force constants for the short-range interactions, we calculate from them potential parameters by assuming pairwise A-O, B-O, and O-O interactions. These are represented by Buckingham potentials: $V(r)=ae^{(-br)}-c/r^6$. Actually, the van der Waals term is included only for the O-O interaction because it is attractive, as it turns out from the force constants. This fact is commonly observed in oxides. The potential parameters obtained for $KNbO_3$ are listed in Table I.

III. RESULTS

First, we compute the underlying static potential for different ionic displacements in $KTaO_3$. The total energy as a function of [001] displacements is shown in Fig. 1 (right panel). For comparison, the energy as a function of [111] displacements is also shown in the left panel. As it was expected, the cubic structure remains favored over all possible displaced structures. A distortion involving ionic displacements according to the eigenvector for the

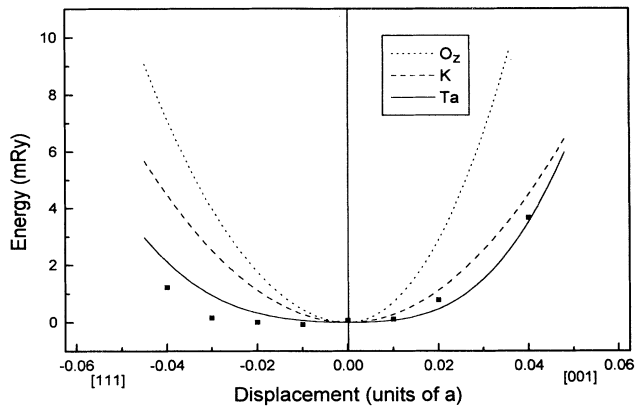

FIG. 1. Total energy versus rhombohedral (left) and tetragonal (right) displacements of K, Ta, and O atoms in $KTaO_3$. The points are the results of Ref. 11 for the Ta displacements, obtained with the experimental lattice constant.

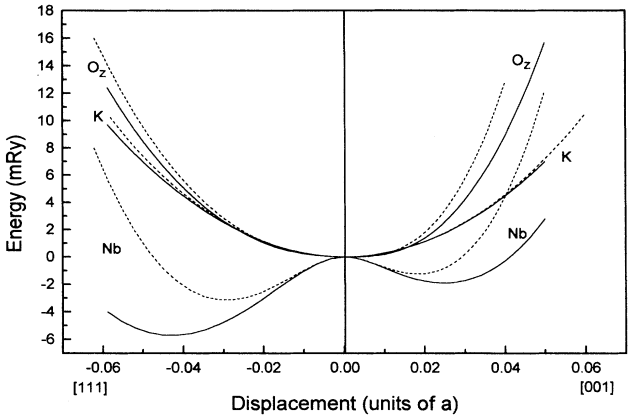

FIG. 2. Total energy versus rhombohedral (left) and tetragonal (right) displacements of K, Nb, and O atoms in $KNbO_3$; solid line, Harmonic potential; dashed line, Buckingam potential.

ferroelectric mode produces only an energy gain of 0.05 mRy and, therefore, the quantum fluctuations are sufficient to stabilize the cubic structure, as it has been shown in the self-consistent phonon calculations.[17,18]

The equilibrium ground-state structure for $KTaO_3$ and $KNbO_3$ were recently studied by the full-potential linear muffin-tin orbital method.[11] It is interesting to point out that the results shown in Fig. 1 are in excellent agreement with the total-energy behavior under various displacements calculated by Postnikov *et al.* To illustrate this, the results of Ref. 11 for Ta displacements, obtained for the experimental lattice constant, are shown in Fig. 1. This agreement means that the nonlinear polarizability model, even in the harmonic approximation for the short-range and Coulomb interactions, describes quite well the anharmonicity of the total-energy surface in $KTaO_3$. It is clear that the anharmonic contribution to this underlying potential comes only from the fourth-order term in the core-shell interaction for the oxygen ion. Thus the nonlinear core-shell coupling at the oxygen ion generates effective quartic interionic potentials in a nontrivial way, which are visualized in Fig. 1. The effective quartic coupling constants had been evaluated in Ref. 22.

For $KNbO_3$. we perform a similar analysis of the total-energy behavior. As it was mentioned, the model for $KNbO_3$ is obtained by changing only two parameters which describe the linear and nonlinear oxygen polarizability. The total energy as a function of [001] and [111] displacements of the Nb^{+5}, K^{+}, and O_z^{-2} sublattices is shown in Fig. 2. It is clear that the cubic structure is unstable under the Nb displacements. A similar instability with an energy minimum of ≈ -3.8 mRy is obtained for Nb displacements along a [110] direction. If all ions are simultaneously displaced according to the ferroelectric mode the energy behaves quite similar to the curves corresponding to Nb displacements, with only slightly lower minimums. The displacement along the [111] direction results in a deeper total-energy minimum, which is consistent with the fact that the low-temperature ferroelectric state of $KNbO_3$ has rhombohedral symmetry. The Nb shift along this direction is ≈ 0.18 Å which is in fairly good agreement with 0.21 Å obtained by an EXAFS analysis.[9] Also the relative values of the minimums along [001] and [110] directions are consistent with the sequence of the different structural transitions.

To check the validity of the harmonic approximation for the short-range and Coulomb interactions, we compare the total-energy surface obtained with the potential in Eq. (1) with the one calculated with the short-range Buckingham potentials (see Table I) and the true Coulomb interactions. The latter is treated with the usual Ewald procedure. The results are also shown in Fig. 2. As expected, the exponential growth of the repulsive interaction leads to a less deep well for Nb, and in general a faster growth of the energy at large ionic displacements. However, the potential leads to a qualitative behavior of the total energy very similar to the harmonic approximation, including the sequence of energy minimums for Nb displacements along the three symmetry axes. It is worthwhile to point out that very small variations of the cubic lattice constants produce large effects on the energy curves corresponding to the Buckingham potentials.

In Fig. 3 we compare our results will recent model calculations[10] and total-energy studies using local-density approximation.[11] We observe a qualitative agreement in spite of the simplicity of our model. Taking into account the large quantitative differences between the various results, which are of the order of the precision in first-

TABLE I. Short-range potential parameters for $KNbO_3$.

Interaction	a (eV)	b (A^{-1})	c (eV A^6)
K-O	124 189.4	0.3516	0.0
Nb-O	1 131.3	0.4972	0.0
O-O	3 576.9	0.3516	833.5

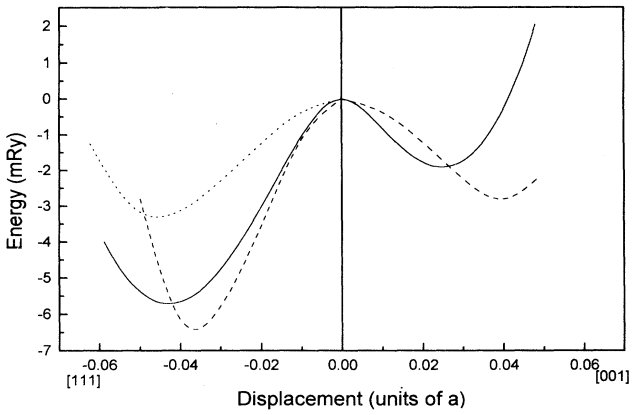

FIG. 3. Total energy versus rhombohedral displacement (left) and tetragonal (right) of Nb in $KNbO_3$. Solid line, nonlinear polarizability model; dashed line, from Ref. 10 and dotted line, from Ref. 11.

principle calculations ($\approx$mRy), and the strong volume dependence of the energy wells observed in both *ab initio*[11] and model potential calculations, we find no reason to give more confidence to one of these results. Therefore the harmonic approximation for the short-range interactions, which also gives a good qualitative agreement with the other results, can be considered as a good starting point for simulations of the dynamical behavior across the transitions.

Finally, we apply our model to analyze whether the tetragonal and the orthorhombic phases correspond to saddle points on the total-energy surface, or whether there are local energy minimums. To this purpose, we evaluate the total energy for Nb displacements in a plane which contains the [001], [110], and [111] directions and the results are plotted in Fig. 4. As can be seen there, the energy minimums of the tetragonal and orthorhombic phases are indeed saddle points. This feature indicates that the nonlinear polarizability model, besides describing the softening of the ferroelectric modes, also gives support to the eight-site model.

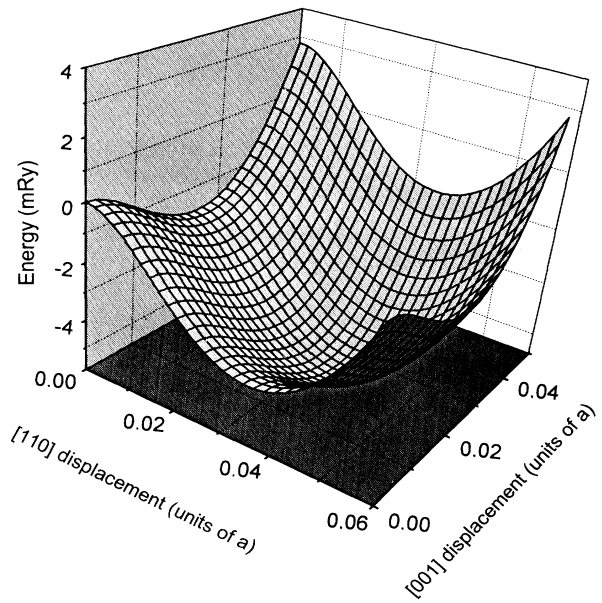

FIG. 4. Total-energy surface for Nb displacements on a (110) plane.

IV. DISCUSSION

From recent first-principles calculations of the electronic structure of several ABO_3 perovskites it has been concluded that the *p-d* hybridization between oxygen and the *B* transition-metal ion should be more important than the oxygen polarizability for the ferroelectric transition. Due to this hybridization, a significant amount of electronic charge flows from the oxygen towards the B ion during the ferroelectric distortion.[12,26] This effect actually does not contradict, but rather supports the phenomenological description of polarizabilities made in the shell model with anisotropic nonlinear oxygen polarizability. The shell model accounts for the electronic polarizability effects in the lattice dynamics by generating a dipole at each ionic site. These are the centers of highest charge density in the ABO_3 perovskites even in the presence of an important *p-d* hybridization, since the charge-density maps do not display the overlap charge maximums which justify the application of the bond-charge model for the covalent crystals. However, the polarizabilities attached to the oxygen or the B ion are not intrinsic properties of these ions; they include hybridization effects. As the nonlinear oxygen polarizability model was developed,[17,23] it has been already suggested that the oxygen polarizability component along the B-O bond should be dynamically enhanced by the *p-d* hybridization.

Also the positive B ion shell charge in our model for $KTaO_3$ and $KNbO_3$ contributes to simulate the mentioned flow of electronic charge from oxygen to the B ion. In fact, by performing the ferroelectric displacement pattern, we observe that a displacement of the oxygen shell towards one of its B neighbors induces an opposite displacement of this neighbor shell. Thus both ions develop dipoles with opposite sense to the oxygen shell displacement, which describes in a dipolar approximation a net flow of electronic charge from oxygen to the B ion.

In order to further test the ability of our model to describe electronic polarization effects, we have calculated the dynamical Born effective charges $\tilde{Z}(\kappa)$ for comparison with recent first-principles calculations.[24–26] These charges determine the lattice dynamical contribution to the dielectric constant through

$$\epsilon_{\alpha\beta}(\omega)=\epsilon_{\alpha\beta}(\infty)+\frac{4\pi}{\Omega}\sum_j \frac{p_\alpha^*(j)p_\beta(j)}{\omega_j^2-\omega^2-i\omega\Gamma_j(\omega)} , \quad (3)$$

where j denotes TO modes at $\mathbf{q}=0$ and

$$p_\alpha(j)=|e|\sum_\kappa \tilde{Z}_\alpha(\kappa)\frac{e_\alpha^\kappa(j)}{\sqrt{m_\kappa}} . \quad (4)$$

Here $e_\alpha^\kappa(j)$ are the normalized eigenvectors of the dynamical matrix and m_κ the ionic masses. Due to site symmetry in the cubic phase, for the A and B ions $\tilde{Z}(\kappa)$ is isotropic, but $\tilde{Z}(O)$ is a diagonal tensor with a different component along the O-B direction than in the plane where the oxygen is surrounded by four A ions. The shell model expression for $\tilde{Z}(\kappa)$ is[27]

$$\tilde{Z}_\alpha(\kappa)=Z(\kappa)+\sum_{\kappa'} Y(\kappa')\mathcal{F}_{\kappa'\kappa}^{\alpha\alpha}\ , \tag{5}$$

where

$$\mathcal{F}=(\mathcal{S}+\mathcal{H}_2+\mathcal{C}^{YY})^{-1}(\mathcal{S}+\mathcal{C}^{ZY})^{\dagger}\ . \tag{6}$$

The second term in Eq. (5) is the electronic polarizability contribution to the effective charge. With the model parameters for $KNbO_3$ we obtain $\tilde{Z}(K)=1.06$, $\tilde{Z}(Nb)=8.25$, $\tilde{Z}_z(O_z)=-6.19$, and $\tilde{Z}_y(O_z)=\tilde{Z}_x(O_z)=-1.57$, where O_z denotes an oxygen with the Nb neighbors along z. These values are in quite good agreement with those arising from first-principles calculations.[25,26] In these works it is shown that the huge values of $\tilde{Z}(Nb)$ and $\tilde{Z}_z(O_z)$ stem from the O $2p$–Nb $4d$ hybridization. We conclude that the corresponding electronic polarization effects are quite good simulated by our shell model.

We now turn to the nonlinear part of the oxygen polarizability, i.e., the anisotropic variation of this property with the B-O distance. One could question the assignation of this nonlinearity to the oxygen and not to the B ion, whose d orbitals contribute as well to the electronic polarizability. This dilemma is very difficult to solve unambiguously from the *ab initio* results on the charge-density redistributions due to variations of the B-O bond length. Therefore we prefer to recall the phenomenological basis of the model given in the past, which is further supported by the present results. The nonlinearity at the oxygen not only explains the softening of the ferroelectric mode but also the phonon temperature dependences in the whole spectrum measured on a wide range of temperatures in $KTaO_3$.[18] It has been speculated[28] that a more pronounced charge transfer in $KNbO_3$ would cause the oxygen ions to become less polarizable than in $KTaO_3$, while the Nb ions should be more polarizable than the Ta ions. This is contrary to our model simulation of the hybridization effects through an enhancement of the oxygen polarizability. It is in addition argued that a variation of the Nb polarizability drives the ferroelectric instability in $KNbO_3$. We observe the analogous effect in $KTaO_3$, but a variation of the Ta polarizability produces phonon shifts which disagree with the experience. A strong argument in favor of the oxygen nonlinearity is also that it leads to a second-order Raman spectrum in very good agreement with the measurement in $KTaO_3$.[18] Also the Raman spectrum of $KTa_{1-x}Nb_xO_3$ is well reproduced by the model.[20] The Raman tensor is expressed as a quadratic combination of functions of the shell normal displacements where the combination coefficients are related to the nonlinear coupling constants. The calculations of the Raman tensor is then a very sensitive test of both the phonon eigenvectors and frequencies over the whole Brillouin zone and of the polarizability mechanism chosen.

As a general conclusion of the above discussion, we remark that the *p-d* hybridization and the nonlinear oxygen polarizability are not contradictory view points for the explanation of the origin of ferroelectricity in the perovskites.[29] On the contrary, we have shown that the model simulates adequately the polarization effects arising from that hybridization.

Finally, we have shown in this paper that the oxygen nonlinearity allows us to simulate quite satisfactory the *ab initio* underlying potential for the relevant ionic displacements which lead to the series of ferroelectric transitions in $KNbO_3$. When treated in the self-consistent phonon approximation, the model describes correctly the lattice dynamics and the ferroelectric soft mode. However, when approaching the transitions, an exact treatment of the underlying potential is needed, which will lead to an order-disorder dynamics as proposed for the eight-site model. Thus the model is expected to be able to explain the experimentally observed crossover from a soft-mode to an order-disorder behavior near the transition. A preliminary simulation with a drastically simplified two-dimensional (2D) version of the model supports this expectation.[21] A molecular-dynamics simulation with the present realistic 3D model is in progress.

ACKNOWLEDGMENTS

We thank A. Dobry for many clarifying discussions and comments. This work was supported by Consejo Nacional de Investigaciones Científicas y Técnicas de la República Argentina. M.G.S. acknowledges support from Consejo de Investigaciones de la UNR.

[1] A. W. Hewat, J. Phys. C **6**, 2559 (1973).
[2] W. Cochran, Adv. Phys. **9**, 387 (1960).
[3] M. D. Fontana, G. Métrat, J. Servoin, and F. Gervais, J. Phys. C **16**, 483 (1984), and references therein.
[4] R. Comes, R. Lambert, and A. Guinier, Solid State Commun. **6**, 715 (1968); Acta Crystallogr. Sect. A **26**, 244 (1970).
[5] S. Chaves, F. C. S. Barreto, R. A. Nogueira, and B. Zēks, Phys. Rev. B **13**, 207 (1976).
[6] K. A. Müller and W. Berlinger, Phys. Rev. B **34**, 6130 (1986).
[7] J. P. Sokoloff, L. L. Chase, and D. Rytz, Phys. Rev. B **38**, 597 (1988).
[8] M. D. Fontana, A. Ridah, G. E. Kugel, and C. Carabatos-Nedelec, J. Phys. C **21**, 5853 (1988).
[9] N. de Mathan, E. Prouzet, E. Husson, and H. Dexpert, J. Phys. Condens. Matter **5**, 1261 (1993).
[10] P. Edwardson, Phys. Rev. Lett. **63**, 55 (1989).
[11] A. Postnikov, T. Neumann, G. Borstel, and M. Methfessel, Phys. Rev. B **48**, 5910 (1993).
[12] R. Cohen and H. Krakauer, Phys. Rev. B **42**, 6416 (1990).
[13] R. Cohen, Nature **358**, 136 (1992).

[14]D. Singh and L. Boyer, Ferroelectrics **136**, 95 (1992).
[15]R. D. King-Smith and D. Vanderbilt, Phys. Rev. B **49**, 5828 (1994).
[16]W. Zhong, D. Vanderbilt, and K. Rabe, Phys. Rev. Lett. **73**, 1861 (1994).
[17]R. Migoni, H. Bilz, and D. Bäuerle, Phys. Rev. Lett. **37**, 1155 (1976).
[18]C. Perry, R. Currat, H. Buhay, R. Migoni, W. Stirling, and J. Axe, Phys. Rev. B **39**, 8666 (1989).
[19]G. E. Kugel, M. D. Fontana, and W. Kress, Phys. Rev. B **35**, 813 (1987).
[20]G. E. Kugel, H. Mesli, M. D. Fontana, and D. Rytz, Phys. Rev. B **37**, 5619 (1988).
[21]M. Stachiotti, A. Dobry, R. Migoni, and A. Bussmann-Holder, Phys. Rev. B **47**, 2473 (1993).
[22]R. Migoni, H. Bilz, and D. Bäuerle, in *Lattice Dynamics,* edited by M. Balkanski (Flammarion Sciences, Paris, 1978), p. 650.
[23]A. Bussmann, H. Bilz, R. Roenspiess, and K. Schwarz, Ferroelectrics **25**, 343 (1980).
[24]R. Resta, M. Posternak, and A. Baldereschi, Phys. Rev. Lett. **70**, 1010 (1993).
[25]W. Zhong, R. D. King-Smith, and D. Vanderbilt, Phys. Rev. Lett. **72**, 3618 (1994).
[26]M. Posternak, R. Resta, and A. Baldereschi, Phys. Rev. B **50**, 8911 (1994).
[27]H. Chen and J. Callaway, Phys. Rev. B **45**, 2085 (1992).
[28]H. Donnerberg and M. Exner, Phys. Rev. B **49**, 3746 (1994).
[29]A. Bussmann-Holder and H. Buttner, Nature **360**, 540 (1992); R. Cohen, *ibid.* **362**, 213 (1993).

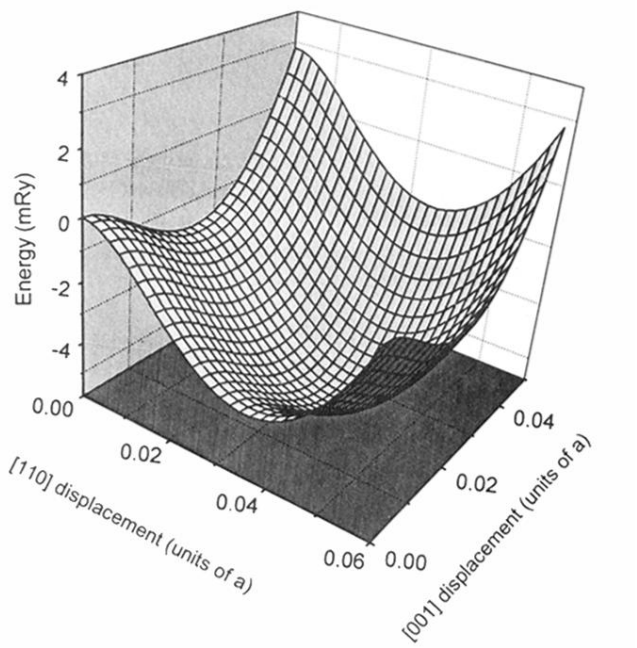

FIG. 4. Total-energy surface for Nb displacements on a (110) plane.